Recombinase-activating gene (RAG) 2-mediated V(D)J recombination is not essential for tumorigenesis in *Atm*-deficient mice

Lisa K. Petiniot*†‡, Zoë Weaver‡§, Carrolee Barlow‡¶‖, Rhuna Shen*†‡, Michael Eckhaus, Seth M. Steinberg††, Thomas Ried§, Anthony Wynshaw-Boris¶‡‡, and Richard J. Hodes*§§¶¶**

*Experimental Immunology Branch, §Genetics Department, and ††Biostatistics and Data Management Section, Office of the Director of the Division of Clinical Sciences, National Cancer Institute; ¶Genetic Disease Research Branch, National Human Genome Research Institute; **Veterinary Resources Program, Office of Research Services; §§National Institute on Aging, National Institutes of Health, Bethesda, MD 20892; and †Howard Hughes Medical Institute, National Institutes of Health Research Scholars Program, One Cloister Court, Bethesda, MD 20892

Edited by Michael Potter, National Institutes of Health, Bethesda, MD, and approved March 20, 2000 (received for review December 28, 1999)

The majority of *Atm*-deficient mice die of malignant thymic lymphoma by 4–5 mo of age. Cytogenetic abnormalities in these tumors are consistently identified within the *Tcr* α/δ locus, suggesting that tumorigenesis is secondary to aberrant responses to double-stranded DNA breaks that occur during V(D)J recombination. Since V(D)J recombination is a recombinase-activating gene (RAG)-dependent process, we generated *Rag2*$^{-/-}$*Atm*$^{-/-}$ mice to assess the requirement for RAG-dependent recombination in thymic lymphomagenesis. In contrast to expectation, the data presented here indicate that development of malignant thymic lymphoma in *Atm*$^{-/-}$ mice is not prevented by loss of RAG-2 and thus is not dependent on V(D)J recombination. Malignant thymic lymphomas in *Rag2*$^{-/-}$*Atm*$^{-/-}$ mice occurred at a lower frequency and with a longer latency as compared with *Atm*$^{-/-}$ mice. Importantly, cytogenetic analysis of these tumors indicated that multiple chromosomal abnormalities occurred in each tumor, but that none of these involved the *Tcr* α/δ locus. Nonmalignant peripheral T cells from TCR-transgenic *Rag2*$^{-/-}$*Atm*$^{-/-}$ mice also revealed a substantial increase in translocation frequency, suggesting that these translocations are early events in the process of tumorigenesis. These data are consistent with the hypothesis that the major mechanism of tumorigenesis in *Atm*$^{-/-}$ mice is via chromosomal translocations and other abnormalities that are secondary to aberrant responses to double-stranded DNA breaks. Furthermore, these data suggest that V(D)J recombination is a critical, but not essential, event during which *Atm*-deficient thymocytes are susceptible to developing chromosome aberrations that predispose to malignant transformation.

Ataxia telangiectasia (AT) is an autosomal recessive disease characterized by ataxia, ocular telangiectasias, humoral and cellular immunodeficiencies, increased incidence of cancers, and increased sensitivity to ionizing radiation (reviewed in ref. 1). The genetic defect causing this disease is mutation of the gene encoding the AT mutated (ATM) protein (2). ATM appears to play an important role in cellular responses to the presence of double-stranded DNA (dsDNA) breaks, probably due to its function in cell cycle checkpoint control (3). Several components of the AT phenotype, such as sensitivity to ionizing radiation, infertility, immunodeficiency, and lymphoreticular malignancies with characteristic translocations, plausibly result from aberrant responses to dsDNA breaks. More specifically, it has been suggested that immunodeficiency and the increased incidence of lymphoid cancers seen in this disease are secondary to aberrant recognition and repair of dsDNA breaks that normally occur during V(D)J recombination and isotype switching in lymphoid cells (3, 4).

Support for this hypothesis comes from studies of the murine model of AT. It has been observed that the majority of *Atm*$^{-/-}$ mice die from malignant thymic lymphoma by 4–5 mo of age (5–7). The initial characterization of *Atm*$^{-/-}$ mice demonstrated that these lymphomas displayed translocations detected by spectral karyotyping (SKY) (5), and recent analysis demonstrated that 100% of thymic lymphomas from *Atm*$^{-/-}$ mice had translocations in chromosome 14. Notably, these translocations were shown by fluorescent *in situ* hybridization (FISH) to occur consistently within both alleles of the T cell receptor *(Tcr)* α/δ locus (M. Liayanage, C.B., Z.W., A. Coleman, D. G. Pankratz, S. Anderson, A.W.-B., and T.R., unpublished work). The consistent involvement of the *Tcr* α/δ locus suggests a mechanism of tumorigenesis in which dsDNA breaks occurring within this locus during V(D)J recombination are not efficiently handled in *Atm*-deficient cells during T cell development. The dsDNA breaks and increased chromosomal instability typically seen in AT (reviewed in ref. 1) predispose to development of malignant thymic lymphoma.

In a recent study designed to test this hypothesis, Liao and Van Dyke (8) used the fact that V(D)J recombination is a recombinase-activating gene (RAG)-dependent process and generated *Rag1*$^{-/-}$*Atm*$^{-/-}$ mice to assess tumor incidence. If tumorigenesis is secondary to faulty V(D)J recombination, no tumors would be expected to develop in these double knockout mice. Consistent with this hypothesis, development of malignant thymic lymphoma did not occur in nine *Rag1*$^{-/-}$*Atm*$^{-/-}$ mice, whereas five of five *Rag1*$^{+/-}$*Atm*$^{-/-}$ control mice died of malignant thymic lymphomas by 7 mo of age.

We had independently initiated a similar series of experiments in which we generated *Rag2*$^{-/-}$*Atm*$^{-/-}$ mice for assessment of tumor susceptibility. Surprisingly, in contrast to expectation and the results reported by Liao and Van Dyke (8), we observed development of malignant thymic lymphomas in *Rag2*$^{-/-}$*Atm*$^{-/-}$ mice, although at a lower frequency and with a longer latency than in *Atm*$^{-/-}$ mice. Strikingly, cytogenetic evaluation of these *Rag2*$^{-/-}$*Atm*$^{-/-}$ thymic lymphomas revealed an absence of the *Tcr* α/δ locus translocations that were seen in lymphomas from *Atm*$^{-/-}$ mice with intact RAG function. These findings indicate that rearrangement of the *Tcr* α/δ locus is a critical, but not

This paper was submitted directly (Track II) to the PNAS office.

Abbreviations: AT, ataxia telangiectasia; Atm, ataxia telangiectasia mutated; RAG, recombinase-activating gene; Tcr, T cell receptor; SKY, spectral karyotyping; FISH, fluorescent *in situ* hybridization; ds, double stranded; BAC, bacterial artificial chromosome.

‡L.K.P. and Z.W. contributed equally to this work.

‖Present address: The Salk Institute for Biological Studies, Laboratory of Genetics, 10010 North Torrey Pines Road, La Jolla, CA 92037.

‡‡Present address: University of California, San Diego School of Medicine, 9500 Gilman Drive, La Jolla, CA 92093-0627.

¶¶To whom reprint requests should be addressed at: Building 10, Room 4B10, National Institutes of Health, 10 Center Drive, MSC 1360, Bethesda, MD 20892-1360. E-mail: richard_hodes@nih.gov.

The publication costs of this article were defrayed in part by page charge payment. This article must therefore be hereby marked "*advertisement*" in accordance with 18 U.S.C. §1734 solely to indicate this fact.

essential, event during which *Atm*-deficient thymocytes are susceptible to developing translocations that predispose to malignancy. Furthermore, the data indicate that the role of ATM is not limited to recognition and repair of dsDNA breaks initiated by V(D)J recombination, but rather that ATM functions more broadly in predisposing to translocation events and tumorigenesis.

Materials and Methods

Flow Cytometric Analysis. The following conjugated antibodies were used for three-color flow cytometric analysis: anti-CD8 FITC, anti-Thy 1.2 FITC, anti-CD4 phycoerythrin (Becton Dickinson Immunocytometry Systems), anti-CD3 FITC, anti-B220 phycoerythrin, anti-H57 biotin, and anti-Vβ8 biotin (PharMingen). Anti-Leu-4 FITC, anti-Leu-4 phycoerythrin, and anti-Leu-4 biotin (Becton Dickinson Immunocytometry Systems) were used as negative staining controls. Biotin-conjugated antibodies were revealed with streptavidin-CyChrome (PharMingen). Samples were analyzed on a FACScan (Becton Dickinson Immunocytometry Systems) using CellQuest software.

Breeding and Typing Mice. The creation of *Atm*-deficient mice (allele designation $Atm^{ins5790neo}$) has been described previously (5). Progeny of heterozygote matings were genotyped by PCR (9). *Rag2*-deficient mice (10) were identified phenotypically by flow cytometric analysis of peripheral blood lymphocytes as described above. $Rag2^{-/-}$ cells were $CD4^-CD8^-B220^-$; $Rag2^+$ cells were $CD4^+$, $CD8^+$, or $B220^+$. To generate mice deficient for both *Rag2* and *Atm,* double heterozygotes were crossed and progeny were typed as described above. To create $HyTcrTg^+Rag2^{-/-}Atm^{-/-}$ mice, $HyTcrTg^+$ mice (11) were first crossed with $Rag2^{-/-}Atm^{+/-}$ mice. These mice were typed for the presence of transgene by flow cytometric analysis as described above. Peripheral blood lymphocytes from $HyTcrTg^+Rag2^{-/-}$ mice were $B220^-$, but had a population of Thy $1.2^+V\beta8^+$ cells, whereas peripheral blood lymphocytes from $HyTcrTg^-Rag2^{-/-}$ mice were Thy 1.2^-B220^-. $HyTcrTg^+Rag2^{-/-}Atm^{+/-}$ mice were then crossed with $HyTcrTg^-Rag2^{-/-}Atm^{+/-}$ mice.

Tumor Incidence Studies and Histopathological Analysis. Mice were examined daily for evidence of morbidity or mortality. Mice were killed when death was judged to be imminent; thoracic and abdominal organs were removed *en bloc* and preserved in 10% neutral buffered Formalin (Sigma) for necropsy. Organs from mice that were found dead were similarly preserved. Fixed tissues were embedded in paraffin blocks, sectioned, and stained with hematoxylin and eosin by American Histology Labs (12), and sections were examined by light microscopy.

Statistical Analysis. Survival time of mice was calculated from date of birth until date of death or date last known alive. All animals in which death was felt to be imminent were killed, and the underlying morbidity was recorded as the cause of mortality. Kaplan-Meier survival curves were generated separately for death due to malignant thymic lymphoma and death due to malignancy other than malignant thymic lymphoma (13). Animals were considered to have failed in the analysis of a given end point if a diagnosis of that end point was made; animals that died due to a cause other than that end point had their follow-up time censored in that curve at the date of death. Three mice were excluded from analysis because their survival durations were unknown. The statistical significance of differences between pairs of Kaplan–Meier curves, each representing a different group of animals, was determined by the Mantel–Haenszel method (14). Individual, unadjusted *P* values are reported and all were determined to indicate statistical significance at the 0.05 level in view of the multiple comparisons being made according to the method of Hochberg (15). All *P* values are two-tailed.

Thymic Lymphoma Cell Culture. Thymic lymphomas were harvested and single-cell suspensions were cultured in RPMI 1640 (BioWhittaker) supplemented with 15% FCS (Biofluids, Rockville, MD), sodium pyruvate (1%), nonessential amino acids (1%), L-glutamine (0.5%), 2-mercaptoethanol (5×10^{-5}), penicillin (0.5%), streptomycin (0.5%), and either 20 IU/ml human recombinant IL-2 ($Atm^{-/-}$ lymphomas) or 100 IU/ml human recombinant IL-2 and 6 ng/ml rmIL-7 ($Rag2^{-/-}Atm^{-/-}$ lymphomas).

SKY and FISH. Metaphase chromosomes were prepared from tumor cell lines at early passage numbers (passages 0–2). Cells were incubated in 0.1 μg/ml Colcemid (GIBCO/BRL) for 30–60 min and then lysed in 0.075 M KCl. Chromosomes were fixed in 3:1 methanol:acetic acid and dropped onto glass slides. Thymocyte chromosomes were prepared by culturing single-cell thymocyte suspensions for 2 h in 0.1 μg/ml Colcemid and then lysing and fixing as described above. Splenocyte chromosomes were prepared from splenocytes cultured for 48 h in RPMI 1640 + 20% FCS with 6 μg/ml concanvalin A to preferentially stimulate T cells. After an additional 30-min incubation in 0.1 μg/ml Colcemid, cells were harvested and metaphase chromosomes were prepared as described. SKY of the tumor cell lines was performed as described previously (16, 17). Raw spectral images were visualized by assigning red, green, or blue colors to specific spectral ranges. Chromosomes were then unambiguously identified using a spectral classification algorithm that results in the assignment of a separate classification color to all pixels with identical spectra by use of Sky View software (Applied Spectral Imaging). Aberrations were defined using the nomenclature rules from the Committee on Standardized Genetic Nomenclature for Mice (see the Mouse Genome Informatics web site at http://www.informatics.jax.org). Six to 10 metaphases were analyzed for each tumor, and 10–12 metaphases were analyzed for each splenocyte or thymocyte preparation. Bacterial artificial chromosome (BAC) clones for FISH analysis were labeled by nick-translation with biotin-dUTP (Cα) and Spectrum Orange-dUTP (Vα and Cδ), whereas the whole chromosome 14 paint was labeled with digoxin-dUTP and detected with mouse anti-digoxin followed by sheep anti-mouse IgCy5.5. FISH results were imaged and analyzed using QFISH software (Leica, Cambridge, U.K.).

Results

Incidence of Malignant Thymic Lymphomas in Mice Deficient in Both ATM and RAG-2. To determine whether tumorigenesis in *Atm*-deficient mice is dependent on V(D)J recombination, we intercrossed $Rag2^{+/-}Atm^{+/-}$ mice to generate $Rag2^{-/-}Atm^{-/-}$ mice and littermate controls as described in *Materials and Methods*. Kaplan–Meier analysis of tumor-free survival was determined. If tumorigenesis is secondary to aberrant recognition of dsDNA breaks that occur during V(D)J recombination of the *Tcr* α/δ locus, it would be expected that preventing V(D)J recombination by deleting the *Rag2* gene would prevent the development of malignant thymic lymphoma in $Rag2^{-/-}Atm^{-/-}$ mice.

In contrast to this prediction, however, $Rag2^{-/-}Atm^{-/-}$ mice did in fact develop malignant thymic lymphomas (Fig. 1). Of 24 $Rag2^{-/-}Atm^{-/-}$ mice followed, 6 (25%) were diagnosed with malignant thymic lymphoma at necropsy as compared with 0 of 13 $Rag2^+Atm^{+/+}$ mice ($P = 0.0018$ by Mantel–Haenszel test comparing overall probabilities as a function of time). Age at death ranged from 7–17.5 mo, with the mean age at death being 12 mo. $Rag2^+Atm^{-/-}$ littermate controls had a higher frequency of tumorigenesis and a shorter latency to tumor development (Fig. 1). Seven of 12 $Rag2^+Atm^{-/-}$ mice (58%) developed malignant thymic lymphoma as compared with 0 of 13 $Rag2^+Atm^{+/+}$ mice ($P = 0.0012$ by Mantel–Haenszel test) or as compared with 6 of 24 $Rag2^{-/-}Atm^{-/-}$ mice ($P = 0.036$ by

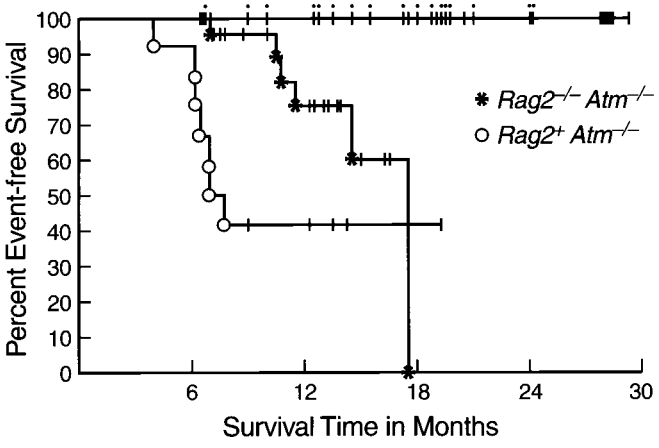

Fig. 1. Kaplan–Meier analysis of tumor incidence studies. Thymic lymphoma-free survival is plotted versus time in months for *Rag2*$^{-/-}$*Atm*$^{-/-}$ mice and littermate controls. A drop in the curve represents the sacrifice or death of an animal diagnosed at necropsy with malignant thymic lymphoma. Tick marks represent the sacrifice or death of an animal that was not subsequently diagnosed with malignant thymic lymphoma. For purposes of statistical analysis *Rag2*$^{-/-}$*Atm*$^{+/+}$ and *Rag2*$^{-/-}$*Atm*$^{+/-}$ mice were considered as one group denoted *Rag2*$^{-/-}$*Atm*$^{+}$ (n = 17); likewise, *Rag2*$^{+}$*Atm*$^{+/+}$ and *Rag2*$^{+}$*Atm*$^{+/-}$ were considered as one group denoted *Rag2*$^{+}$*Atm*$^{+}$ (n = 13). As no animals from either of these groups were diagnosed with malignant thymic lymphomas, the curves for these two groups are at 100% event-free survival. To distinguish between *Rag2*$^{-/-}$*Atm*$^{+}$ and *Rag2*$^{+}$*Atm*$^{+}$ mice, dots above the tick marks were used to indicate the death of *Rag2*$^{-/-}$*Atm*$^{+}$ mice.

Mantel–Haenszel test). Age at death ranged from 4–7.75 mo, with a mean age at death of 6.4 mo.

Since T cell development is arrested at the CD4^{-}CD8^{-} stage in *Rag2*$^{-/-}$ mice (10), it was possible that the occurrence of thymic lymphomas in *Rag2*$^{-/-}$*Atm*$^{-/-}$ mice is related to the developmental arrest in *Rag2*-deficient thymocytes. To test this possibility, we generated *HyTcrTg*$^{+}$*Rag2*$^{-/-}$*Atm*$^{-/-}$ mice, in which the arrest in T cell development due to *Rag2* deficiency is rescued by *Tcr* transgene expression (18), and monitored these mice for development of thymic lymphoma. Preliminary study of *HyTcrTg*$^{+}$*Rag2*$^{-/-}$*Atm*$^{-/-}$ mice revealed that malignant thymic lymphomas do develop in these mice and thus demonstrates that lymphomagenesis in *Atm*-deficient mice is independent of T cell developmental arrest.

In addition to malignant thymic lymphomas, *Atm*-deficient mice also showed an increased incidence of nonthymic tumors as compared with control mice. Seven of 24 *Rag2*$^{-/-}$*Atm*$^{-/-}$ mice (29%) and 2 of 12 *Rag2*$^{+}$*Atm*$^{-/-}$ mice (17%) developed various forms of nonthymic malignancy as compared with 0 of 13 *Rag2*$^{+}$*Atm*$^{+/+}$ mice (P = 0.0134 and P = 0.0072, respectively, by Mantel–Haenszel test). These malignancies included two cases of disseminated lymphoma (*Rag2*$^{-/-}$*Atm*$^{-/-}$ mice), a variety of sarcomas (*Rag2*$^{-/-}$*Atm*$^{-/-}$ and *Atm*$^{-/-}$ mice), and ovarian granulosa cell tumors (*Rag2*$^{-/-}$*Atm*$^{-/-}$ and *Atm*$^{-/-}$ mice). No mice in control groups (*Rag2*$^{-/-}$*Atm*$^{+}$ and *Rag2*$^{+}$*Atm*$^{+}$ mice) developed any malignant tumors. As might be expected, the early morbidity and mortality of *Rag2*$^{-/-}$*Atm*$^{+}$ mice were often attributable to infectious causes such as pneumonia, myocarditis, candidal esophagitis, subcutaneous abscess, or colitis secondary to *Helicobacter* infection. The majority of *Rag2*$^{+}$*Atm*$^{+}$ (8/13) mice were alive when this study was terminated.

Flow Cytometric Analysis of Rag2$^{-/-}$Atm$^{-/-}$ Tumors. Flow cytometric analysis of *Rag2*$^{-/-}$ *Atm*$^{-/-}$ and HyTcrTg^{+}*Rag2*$^{-/-}$*Atm*$^{-/-}$ malignant thymic lymphomas was performed to evaluate surface phenotypes. Although nearly all *Atm*$^{-/-}$ thymic lymphomas have been reported to have a CD4^{+}CD8^{+} phenotype (5–6, 8), analysis of Rag2$^{-/-}$*Atm*$^{-/-}$ tumors revealed variable profiles. All tumors were negative for surface TCR (Cβ and/or CD3) as expected in *Rag2*$^{-/-}$ mice; however, surface expression of CD4 and CD8 differed among tumors (data not shown). One tumor had a CD4^{-}CD8^{-} phenotype (1107); one was primarily CD4^{-}CD8^{-}, with a subpopulation of CD8^{+} cells (2865); one was predominantly CD4^{+} with a subpopulation that was CD4^{+}CD8^{+} (8039); and two tumors were CD4^{+}CD8^{+} (2998, 8097). The *HyTcrTg*$^{+}$*Rag2*$^{-/-}$*Atm*$^{-/-}$ thymic lymphomas analyzed also expressed varying levels of CD4 and/or CD8 and were TCR Vβ8^{+}, consistent with expression of the *HyTcr* transgene (data not shown). All *Rag2*$^{-/-}$ and *HyTcrTg*$^{+}$*Rag2*$^{-/-}$*Atm*$^{-/-}$ thymic lymphomas were Thy 1.2^{+}, verifying that they were of T cell origin.

The expression of CD4 and/or CD8 on the cell surface of multiple *Rag2*$^{-/-}$*Atm*$^{-/-}$ thymic lymphomas was unanticipated as RAG-2 is necessary for V(D)J recombination and is therefore normally required for T cell development past the CD4^{-}CD8^{-} stage (10). These results are similar to the previous finding that CD3^{-}CD4^{+}CD8^{+} thymic lymphomas develop in *Rag1*$^{-/-}$*p53*$^{-/-}$ and *Rag2*$^{-/-}$*p53*$^{-/-}$ mice (19). To further clarify the circumstances under which CD4 and/or CD8 expression might be occurring, we analyzed thymocytes from non-tumor-bearing *Rag2*$^{-/-}$*Atm*$^{-/-}$ mice by flow cytometry. Thymocytes of three *Rag2*$^{-/-}$*Atm*$^{-/-}$ mice had a CD3^{-}CD4^{-}CD8^{-} phenotype as expected in mice with a *Rag2*-deficient background, whereas thymocytes of three other *Rag2*$^{-/-}$*Atm*$^{-/-}$ mice had a

Fig. 2. SKY analysis of a metaphase cell from *Rag2*$^{-/-}$*Atm*$^{-/-}$ thymic lymphoma 2998 displaying chromosome aberrations. The entire metaphase is shown in display colors with arrows indicating aberrant chromosomes next to the pseudocolors generated by spectra-based classification (see *Materials and Methods*). The full karyotype of this metaphase is 40, XX, T(12;15), T(Dp16;12). Note that this representative metaphase for tumor 2998 does not contain every clonal aberration that is described in Table 1.

Table 1. Summary of structural aberrations in *Rag2*$^{-/-}$ *Atm*$^{-/-}$ and *HyTcrTg*$^{+}$*Rag2*$^{-/-}$ *Atm*$^{-/-}$ thymic lymphomas identified by SKY and FISH analysis

Tumor	Genotype	SKY-detected clonal aberrations*	TCR V∝/C∝ FISH†
2593	*Atm*$^{-/-}$	**T(9;14)**‡ **T(12;9)** +15	V/C rearranged
2865	*Rag2*$^{-/-}$ *Atm*$^{-/-}$	T(9;17) **T(12;9)** **T(18;12)** +15	V/C colocalization
1107	*Rag2*$^{-/-}$ *Atm*$^{-/-}$	**T(2;14)** T(7;4) **T(14;2;1)**	V/C colocalization
8097	*Rag2*$^{-/-}$ *Atm*$^{-/-}$	T(17;1) **T(8;14), T(14;8)** +15	V/C colocalization
2998	*Rag2*$^{-/-}$ *Atm*$^{-/-}$	**T(12D-E;15A)** **Dic(12E;15E)** **Dp(14)** T(Dp16;12) T(17;1)	V/C colocalization
8039	*Rag2*$^{-/-}$ *Atm*$^{-/-}$	T(4;9) Is(9;4) **T(12;15)** **Dp(14E–F)** Dp(16) Dp(17) +4 +Del(5) −9	V/C colocalization
3013	*HyTCRTg*$^{+}$ *Rag2*$^{-/-}$ *Atm*$^{-/-}$	**T(14;1)**	V/C colocalization
3021	*HyTCRTg*$^{+}$ *Rag2*$^{-/-}$ *Atm*$^{-/-}$	**T(14;In14;16)**	V/C colocalization

*Structural aberrations were considered clonal if present in two or more metaphases. Gains and losses were considered clonal if present in at least two or three metaphases, respectively. Aberrations involving chromosomes 12 or 14 are shown in bold. At least 10 metaphase cells were analyzed per tumor.

†Rearrangement within the *Tcr* ∝ locus was detected by FISH with two BAC clones, one each from the variable and constant regions of the gene, as described in *Materials and Methods*.

‡T, translocation (the chromosome donating the centromere is listed first); Dic, dicentric chromosome; Dp, duplication of a chromosome segment; Is, insertion (the inserted segment is listed first); Del, interstitial deletion of a chromosome segment; In, an inverted chromosome segment.

CD3^{-}CD4^{-}CD8^{dull} phenotype (data not shown). This unexpected phenotype of dull CD8 expression could signify a bypass in *Rag2*$^{-/-}$*Atm*$^{-/-}$ mice of the blockade in thymocyte development imposed by the absence of RAG-2. Interestingly, nonmalignant thymocytes from *Rag1*$^{-/-}$*p53*$^{-/-}$ and *Rag2*$^{-/-}$*p53*$^{-/-}$ mice have also been shown to have an unexpected CD4^{+}CD8^{+} phenotype (19).

Cytogenetic Analysis of *Rag2*$^{-/-}$*Atm*$^{-/-}$ Tumors. To investigate chromosomal alterations that might contribute to underlying mechanisms of tumorigenesis, we performed cytogenetic analysis on early passage cells cultured from multiple *Rag2*$^{-/-}$*Atm*$^{-/-}$ and *HyTcrTg*$^{+}$*Rag2*$^{-/-}$*Atm*$^{-/-}$ thymic lymphomas. SKY analysis was used to identify chromosome structural aberrations, whereas FISH analysis using gene-specific probes for the variable and constant regions of the *Tcr* ∝/δ locus was carried out to determine the presence or absence of translocations within this locus. SKY analysis of *Rag2*$^{-/-}$*Atm*$^{-/-}$ and *HyTcrTg*$^{+}$*Rag2*$^{-/-}$*Atm*$^{-/-}$ tumors revealed multiple translocations (Fig. 2), with chromosome 14 being involved in several of these tumors (Table 1). However, unlike *Atm*$^{-/-}$ tumors, *Rag2*$^{-/-}$*Atm*$^{-/-}$ and *HyTcrTg*$^{+}$*Rag2*$^{-/-}$*Atm*$^{-/-}$ tumors exhibited colocalization of the variable and constant region *Tcr* ∝/δ locus FISH probes, indicating an absence of translocations within this locus (Fig. 3 and Table 1). Interestingly, although no consistent translocation can be identified in *Rag2*$^{-/-}$*Atm*$^{-/-}$ and/or *HyTcrTg*$^{+}$*Rag2*$^{-/-}$*Atm*$^{-/-}$ tumors studied, every tumor did exhibit a translocation involving either chromosome 14 or chromosome 12, both of which are homologous to human chromosome 14. Moreover, the breakpoints approximate the same band regions (14D and 12D–F) as has been observed in *Atm*$^{-/-}$ tumors (Fig. 2; Table 1). The predilections for translocations within these chromosomes may be related to the conformation of chromatin structure. If the chromatin is in a more open conformation in these regions, as is necessary for efficient V(D)J recombination (20), these loci might be more susceptible to chromosomal translocations.

If the chromosomal abnormalities observed in these *Rag2*$^{-/-}$*Atm*$^{-/-}$ and *HyTcr Tg*$^{+}$*Rag2*$^{-/-}$*Atm*$^{-/-}$ thymic lympho-

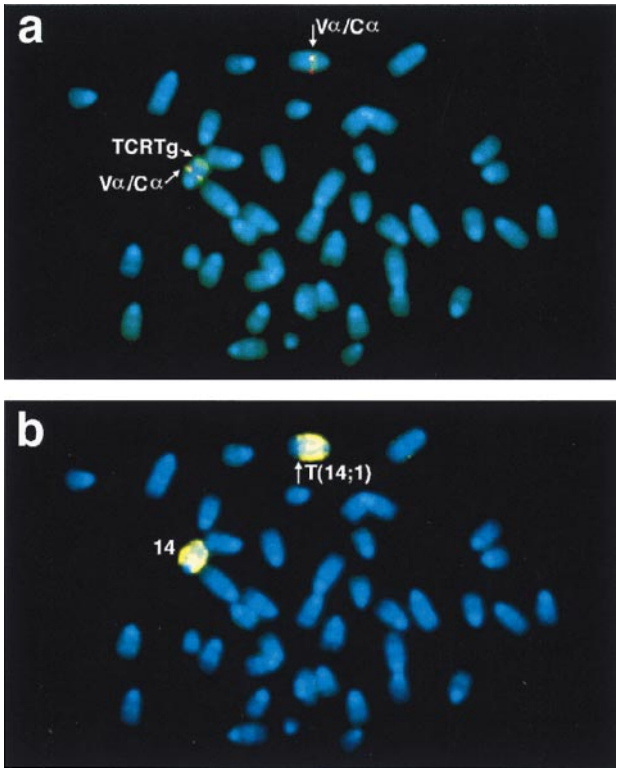

Fig. 3. FISH analysis of the *Tcr* α/δ locus in *HyTcrTg*$^{+}$*Rag2*$^{-/-}$*Atm*$^{-/-}$ thymic lymphoma 3013. (*a*) FISH was performed on tumor 3013 with BAC probes to variable region α (Vα) and constant region α (Cα) in the *Tcr* α/δ locus. The Vα signals are shown in green and the Cα signals are shown in red. Chromosomes are counterstained with 4′,6-diamidino-2-phenylindole (blue). The signals are colocalized, indicating that the *Tcr* α/δ locus is not disrupted. The extra green signal on one chromosome 14 is due to integration of the (prespliced) *HyTcr* transgene (Tg) at that site. (*b*) The same metaphase as in *a* labeled with a chromosome 14 painting probe (yellow), confirming the chromosomal location of the *Tcr* α/δ BAC probes. The chromosome 14 breakpoint in the T(14;1) (indicated by the arrow) is not within the *Tcr* α/δ locus.

Table 2. Chromosome aberrations in *HyTcrTg*$^{+}$*Rag2*$^{-/-}$ *Atm*$^{-/-}$ premalignant thymus and spleen*

Mouse	Genotype	Thymus	Spleen	No. of aberrant metaphases/ total analyzed
8046	*HyTcrTg*$^{+}$ *Rag2*$^{-/-}$ *Atm*$^{-/-}$	T(11;9) T(2;11),T(11;2)	T(3;10),T(3;1) T(12;14) T(12;15)[†] Rb[T(11;9).4][‡] Rb[X.Del(X)]	Thymus: 2/10 = 20% Spleen: 6/12 = 50%
8644	*HyTcrTg*$^{+}$ *Rag2*$^{-/-}$ *Atm*$^{-/-}$	T(12;4)[§] T(12;15;4)[¶]	Not analyzed	Thymus: 8/10 = 80%
8645	*HyTcrTg*$^{+}$ *Rag2*$^{-/-}$ *Atm*$^{+/+}$	None	Not analyzed	Thymus: 0/10 = 0%

*Structural aberrations were determined by SKY analysis. Most aberrations were not clonal (see below for exceptions).
[†]This translocation was present in two metaphase cells.
[‡]Rb, Robertsonian translocation (centromere–centromere dicentric).
[§]This translocation was present in four metaphase cells.
[¶]This translocation was present in four metaphase cells.

mas are early events that occur in precursors of thymic lymphomas and predispose to malignant transformation, one would expect to see similar chromosomal abnormalities in mature T cells from nonmalignant mice of these genotypes. To investigate this possibility, SKY analysis of nonmalignant spleen and thymus T cells from *HyTcrTg*$^{+}$*Rag2*$^{-/-}$*Atm*$^{-/-}$ mice was performed. A high frequency of chromosomal aberrations was observed in two of three mutant mice studied (Table 2). Although most chromosomal aberrations were not clonal, thymocytes from one mouse (8644) did harbor recurrent chromosomal aberrations. No aberrations were found in spleen or thymus T cells from a *HyTcrTg*$^{+}$*Rag2*$^{-/-}$*Atm*$^{+/+}$ mouse (Table 2), and SKY analysis of T cells from wild-type mice did not reveal any chromosome aberrations in over 30 metaphases from three experiments (data not shown).

Discussion

The results of the study reported here clearly indicate that V(D)J recombination is not essential for tumorigenesis; both *Rag2*$^{-/-}$*Atm*$^{-/-}$ and *HyTcrTg*$^{+}$*Rag2*$^{-/-}$*Atm*$^{-/-}$ mice develop malignant thymic lymphomas. Interestingly, however, the thymic lymphomas that develop in *Rag2*$^{-/-}$*Atm*$^{-/-}$ and *HyTcrTg*$^{+}$*Rag2*$^{-/-}$*Atm*$^{-/-}$ mice have distinct characteristics when compared with thymic lymphomas that develop in *Atm*$^{-/-}$ mice. Most importantly, cytogenetic analysis of *Rag2*$^{-/-}$*Atm*$^{-/-}$ and *HyTcrTg*$^{+}$*Rag2*$^{-/-}$*Atm*$^{-/-}$ thymic lymphomas revealed an absence of translocations involving the *Tcr* α/δ locus which are consistently present in *Atm*$^{-/-}$ thymic lymphomas from *Rag2*-competent mice. This finding is consistent with the fact that these tumors originate in mice that lack the RAG-2 protein and therefore cannot generate the dsDNA breaks that initiate V(D)J recombination.

Additionally, *Atm*-deficient mice were found in our study to have an increased incidence of nonlymphoid malignancies as compared with *Atm*-competent mice. The occurrence of malignancies other than thymic lymphomas in *Atm*-deficient mice has not been previously reported, possibly because *Atm*$^{-/-}$ mice die of malignant thymic lymphoma before other types of malignancies have time to develop. In the study reported here, a lower frequency of *Rag2*$^{+}$*Atm*$^{-/-}$ mice (58%) developed malignant thymic lymphoma than was previously reported by Barlow *et al*. (100%; ref. 5). This difference could be the result of differences in genetic background that were created with the introduction of the *Rag2*$^{-/-}$ gene (C57BL/6 background) into *Atm*-deficient mice (129/SvEv background) and/or environmental differences in mouse colonies. It should be noted that, although not as common as lymphomas and leukemias, nonlymphomatous malignancies have also been seen in human patients with AT (21).

The findings reported here help to further define the mechanism by which tumorigenesis occurs in *Atm*-deficient mice. V(D)J recombination is a universal event in thymocyte development that involves the production of dsDNA breaks and which predisposes *Atm*-deficient cells to undergo malignant transformation due to the insertion of oncogenic genes into active TCR loci in T cells (22). However, although V(D)J recombination is a critical event in thymic lymphoma development in *Atm*-deficient mice, our data indicate that it is not essential. In its absence, dsDNA breaks from other causes can predispose *Atm*-deficient cells to undergo malignant transformation, as is evidenced by the occurrence of thymic lymphomas bearing multiple translocations in *Rag2*$^{-/-}$*Atm*$^{-/-}$ mice. The lack of a single type of translocation in *Rag2*$^{-/-}$*Atm*$^{-/-}$ tumors suggests that heterogeneous or stochastic processes are responsible for these dsDNA breaks. As would be expected in such a model, a lower frequency and longer latency of thymic lymphoma development was observed in *Rag2*$^{-/-}$*Atm*$^{-/-}$ mice when compared with *Rag2*$^{+}$*Atm*$^{-/-}$ mice. Additionally, the occurrence of nonlymphomatous malignancies in *Rag2*$^{-/-}$*Atm*$^{-/-}$ and older *Atm*$^{-/-}$ mice is consistent with the model.

Nonmalignant peripheral T cells from *Atm*-deficient mice have been shown to harbor a greater than 20-fold increase in chromosome 14 structural abnormalities as compared with peripheral T cells from wild-type mice (M. Liyanage, C.B., Z.W., A. Coleman, D. G. Pankratz, S. Anderson, A.W.-B., and T.R., unpublished work), suggesting that the translocations within the *Tcr* α/δ locus seen in *Atm*-deficient thymic lymphomas occur early in the process of tumorigenesis. To address the same question in the development of thymic lymphomas in *Rag2*$^{-/-}$*Atm*$^{-/-}$ mice, we analyzed thymocytes from *HyTcrTg*$^{+}$*Rag2*$^{-/-}$*Atm*$^{-/-}$ mice. If the chromosomal structural abnormalities observed in thymic lymphomas from *Rag2*$^{-/-}$*Atm*$^{-/-}$ mice reflect predisposing events in malignant transformation of lymphocytes, we would expect an increased frequency of thymic or peripheral T cells with similar chromosomal aberrations in *HyTcrTg*$^{+}$*Rag2*$^{-/-}$*Atm*$^{-/-}$ mice. Analysis of nonmalignant T cells from *HyTcrTg*$^{+}$*Rag2*$^{-/-}$*Atm*$^{-/-}$ mice indeed revealed multiple chromosome aberrations in thymocytes and splenocytes. These data suggest that the chromosomal structural abnormalities seen in *Rag2*$^{-/-}$*Atm*$^{-/-}$ thymic lymphomas represent early events in the pathway of tumorigenesis and can predispose to selective expansion of lymphocyte clones, as has been observed in the human disease (4, 23).

Because both RAG-1 and RAG-2 are required for V(D)J recombination, with the elimination of either resulting in the absence of V(D)J recombination, one might expect tumor susceptibility in *Rag1*$^{-/-}$*Atm*$^{-/-}$ mice to be similar to that observed in *Rag2*$^{-/-}$*Atm*$^{-/-}$ mice. However, recent results reported by Liao and Van Dyke (8) indicated that malignant thymic lymphomas were not observed in *Rag1*$^{-/-}$*Atm*$^{-/-}$ mice, in marked contrast to the results reported here of tumor occurrence in *Rag2*$^{-/-}$*Atm*$^{-/-}$ mice. This unexpected discrepancy may be accounted for by the fact that the majority of *Rag1*$^{-/-}$*Atm*$^{-/-}$ mice in the study by Liao and Van Dyke (8) died or were killed by 9 mo of age, whereas nearly all of the tumors that developed in *Rag2*$^{-/-}$*Atm*$^{-/-}$ mice in the study described here appeared at a later age. Alternatively, a difference in lymphoma susceptibility between *Rag1*$^{-/-}$*Atm*$^{-/-}$ and *Rag2*$^{-/-}$*Atm*$^{-/-}$ mice could signify previously undescribed differences in RAG-1 and RAG-2 function or could be

attributable to differences in genetic background and/or environmental differences in mouse colonies used in these studies. A comparison of $Rag1^{-/-}Atm^{-/-}$ and $Rag2^{-/-}Atm^{-/-}$ mice has been initiated to address these questions.

We extend sincere thanks for the excellent animal care provided by Genevieve Sanchez, Amy Werling, and the staff at Bioqual, Inc. We are also grateful to Andre Nussenzweig and Al Singer for careful reading of this manuscript and constructive comments.

1. Shiloh, Y. (1995) *Eur. J. Hum. Genet.* **3,** 116–138.
2. Savitsky, K., Bar-Shira, A., Gilad, S., Rotman, G., Ziv, Y., Vanagaite, L., Tagle, D. A., Smith, S., Uziel, T., Sfez, S., *et al*. (1995) *Science* **268,** 1749–1753.
3. Lavin, M. F. & Shiloh, Y. (1997) *Annu. Rev. Immunol.* **15,** 177–202.
4. Taylor, A. M. R., Metcalfe, J. A., Thick, J. & Mak, Y.-F. (1996) *Blood* **87,** 423–438.
5. Barlow, C., Hirotsune, S., Paylor, R., Liyanage, M., Eckhaus, M., Collins, F., Shiloh, Y., Crawley, J. N., Ried, T., Tagle, D., e*t al*. (1996) *Cell* **86,** 159–171.
6. Xu, Y., Ashley, T., Brainerd, E. E., Bronson, R. T., Meyn, M. S. & Baltimore, D. (1996) *Genes Dev.* **10,** 4211–2422.
7. Elson, A., Wang, Y., Daugherty, C. J., Morton, C. C., Zhou, F., Campos-Torres, J. & Leder, P. (1996) *Proc. Natl. Acad. Sci. USA* **93,** 13084–13089.
8. Liao, M.-J. & Van Dyke, T. (1999) *Genes Dev.* **13,** 1246–1250.
9. Liao, M.-J., Yin, C., Barlow, C., Wynshaw-Boris, A. & Van Dyke, T. (1999) *Mol. Cell. Biol.* **19,** 3095–3102.
10. Shinkai, Y., Rathbun, G., Lam, K.-P., Oltz, E. M., Stewart V., Mendelsohn, M., Charron, J., Datta, M., Young, F., Stall, A. M., *et al*. (1992) *Cell* **68,** 855–867.
11. Kisielow, P., Blühthmann, H., Staerz, U. D., Steinmetz, M. & von Boehmer, H. (1992) *Nature (London)* **333,** 742–746.
12. Luna, L. G. (1992) *Histopathological Methods and Color Atlas of Special Stains and Tissue* (American Histolabs, Inc. Publications Division, Gaithersburg, MD).
13. Kaplan, E. & Meier, P. (1958) *J. Am. Stat. Assoc.* **53,** 457–481.
14. Mantel, N. (1966) *Cancer Chem. Rep.* **50,** 163–170.
15. Hochberg, Y. (1988) *Biometrika* **75,** 800–802.
16. Weaver, Z. A., McCormack, S. J., Liyanage, M., duManoir, S., Coleman, A., Schrock, E., Dickson, R. B. & Ried. T. (1999) *Genes Chromosomes Cancer* **25,** 251–260.
17. Liyanage, M., Coleman, A., du Manoir, S., Veldman, T., McCormack, S., Dickson, R. B., Barlow, C., Wynshaw-Boris, A., Janz, S., Wienberg, J., *et al.* (1996) *Nat. Genet.* **14,** 312–315.
18. von Boehmer, H. (1990) *Annu. Rev. Immunol.* **8,** 531–556.
19. Nacht, M. & Jacks, T. (1998) *Cell Growth Differ.* **9,** 131–138.
20. Cherry, S. R. & Baltimore, D. (1999) *Proc. Natl. Acad. Sci. USA* **96,** 10788-10793.
21. Morrell, D., Cromartie, E. & Swift, M. (1986) *J. Natl. Cancer Inst.* **77,** 89–92.
22. Hiom, K., Melek, M. & Gellert, M. (1998) *Cell* **94,** 463–470.
23. Hecht, F., McCaw, B. K. & Koler, R. D. (1973) *N. Engl. J. Med.* **289,** 286–291.